JBC Papers in Press. Published on August 20, 2002 as Manuscript M205361200

Rescue of Embryonic Epithelium Reveals that the Homozygous Deletion of the Retinoblastoma Gene Confers Growth factor Independence and Immortality, but does not Influence Epithelial Differentiation or Tissue Morphogenesis

Kathleen C. Day[1], Michael T. McCabe[1], Xin Zhao[1], Yuzhuo Wang[3,6], Joanne N. Davis[1], John Phillips[4], Marion Von Gelden[4], Thomas Ried[4], Mark A. KuKuruga[2], Gerald R. Cunha[3], Simon W. Hayward[5] and Mark L. Day[1,*]

Running Title: Rb deletion and epithelial physiology and differentiation.

[*Key Words*: retinoblastoma (*Rb)*; tissue recombination (TR) and cellular recombination; epithelial; prostate; Spectral Karyotype (SKY)]

[1]Department of Urology, [2]Flow Cytometry Core, University of Michigan Comprehensive Cancer Center, University of Michigan, Ann Arbor, MI 48109; [3]Department of Anatomy, University of California, San Francisco, CA 94143; [4]The Urologic Oncology Branch/Section of Genetics, National Cancer Institute, National Institutes of Health, Bethesda, MD 20892; [5]Department of Urologic Surgery, Department of Cancer Biology, Vanderbilt-Ingram Comprehensive Cancer Center, Vanderbilt University Medical Center, Nashville, TN 37232; [6]Current address; Department of Cancer Endocrinology, BC Cancer Agency, Canada.

[*]Corresponding author.
University of Michigan
ph: 734-763-9968
fax: 734-647-9271
email: mday@umich.edu

SUMMARY. The ability to rescue viable prostate precursor tissue from retinoblastoma deficient (*Rb-/-*) fetal mice has allowed for the isolation and characterization of the first *Rb-/-* prostate epithelial cell line. This cell line, designated Rb-/-PrE, was utilized for experiments examining the consequences of *Rb* loss on an epithelial population. These findings demonstrated that *Rb* deletion has no discernible effect on prostatic histodifferentiation in Rb-/-PrE cultures. When Rb-/-PrE cells were recombined with embryonic rat urogenital mesenchyme and implanted into athymic male, nude mouse hosts, the recombinants developed into fully differentiated and morphologically normal prostate tissue. The Rb-/-PrE phenotype was characterized by serum-independence in culture and immortality *in vivo*, when compared to wild type controls. Cell cycle analysis revealed elevated S-phase DNA content accompanied by increased expression of cyclin E1 and proliferating cell nuclear antigen (PCNA). Rb-/-PrE cultures also exhibited a diminished ability to growth arrest under high-density culture conditions. We believe that the development of Rb-/- prostate tissue and cell lines has provided a unique experimental platform with which to investigate the consequences of Rb deletion in epithelial cells under various physiological conditions. Additionally, the development of this technology will allow similar studies in other tissues and cell populations rescued from *Rb-/-* fetuses.

INTRODUCTION

The *Rb* gene product mediates numerous cellular functions including cell cycle regulation (1,2), maintenance of chromosomal integrity (3,4), cellular differentiation (5-7), and the survival of epithelial cells (8-11). The *Rb* gene encodes a phosphoprotein (pRb) that regulates the transition between G_1 and S phases of the cell cycle by transducing growth-inhibitory signals that arrest cells in G_1 (12-14). Functional regulation of pRb is cell cycle-dependent, being strictly controlled by the activity of cyclin-dependent kinases that regulate the state of pRb phosphorylation. Dephosphorylated pRb inhibits the transcription of genes via its interaction with members of the E2F family of transcription factors. As the cell approaches the G_1-S border, cyclin D/cdk4/6 and cyclin E/cdk2 complexes sequentially phosphorylates pRb. These events lead to the release of E2F and subsequent activation of E2F-regulated genes such as c-*myc*, cyclin E, PCNA and DNA polymerase, that are required for entry and activation of S-phase.

The control of G_1-S transit provides a dogmatic view of pRb function, as cell cycle regulation is vastly more complex than the simple scheme provided here. The overlapping function of two structurally related family members, p107 and p130, represents an interactive mechanism in which pRb, p107 and p130 share the ability to regulate different members of the E2F family and thus a variety of target genes (13,15,16). Although structurally similar, there is growing evidence supporting distinct cellular functions for each *Rb* family member. All three proteins are differentially expressed during mouse development (17) and their ability to initiate growth arrest is cell-type specific (18). In addition, these proteins preferentially associate with different E2F family members. While pRb interacts with E2F1, 2, 3 and 4 there is apparent redundancy in the regulation of both E2F4 and E2F5 by p107 and p130, reviewed in (19). The similarities and differences between these proteins are also apparent in mice carrying single or

compound knockouts of *Rb*, p107 and p130. When the *Rb* gene is deleted through targeted disruption, the embryos die at 13 days of gestation from defective development of erythroid and neuronal tissues (9,10)-(11). In stark contrast, targeted disruption of either p107 or p130 does not result in an obvious phenotype and the mice remain viable (20).

Members of the *Rb* family are believed to play active roles in tissue development by regulating a postmitotic state required for cellular differentiation (5,20,21). The normal differentiation and development of the prostate gland is critically dependent upon androgenic steroids which, following binding to the androgen receptor, transactivates or represses a number of transcriptional targets, including cell cycle regulatory genes. It was recently demonstrated that pRb is activated during androgen-stimulated epithelial proliferation and during androgen ablation-induced apoptosis (8,22-24). The pRb protein has also been shown to function as a transcriptional co-activator of the androgen receptor (25). Taken together, these results tentatively position *Rb* as a central mediator of androgen action controlling the differentiation, growth and death of prostate epithelium; however, this hypothesis has not been tested.

Cell culture models currently available to study epithelial physiology have a limited scope of relevance with regard to the pRb pathway. Many transformed prostate cell lines, such as DU145, already exhibit nonfunctional pRb due to mutation (26,27). Viral oncogenes are common tools used to immortalize cells in culture or study cell cycle regulatory mechanisms. The viral oncogenes SV-40 large T Antigen, Adenovirus E1A and E1B and HPV E6 and E7 target and inactivate the pocket protein family members (pRb, p107 and p130) as well as p53 (28-30). The use of viral oncogenes has provided substantial insight into the function of the Rb family members and their roles in regulating cell cycle, cell growth and differentiation, however, viral oncogenes are promiscuous in their interactions with other cellular proteins and promote

genomic instability making interpretation of these experimental models difficult. The chromosomal imbalances directly influenced by viral oncogenes have been identified as either random or nonrandom genetic events and include gross chromosomal translocations (31-33). Therefore, models that specifically target and inactivate *Rb*, that minimize complicating genetic alterations inherent with viral oncogenes, might provide novel insight into the physiologic role of *Rb* in epithelial cells.

The homozygous deletion of the *Rb* gene results in embryonic lethality due to a variety of developmental abnormalities (9-11). The embryonic lethality of the *Rb* knockout mutation has prevented the development of *Rb-/-* epithelial cell lines and thus, many of the functional aspects of pRb have not been independently characterized in this cellular population. Recently, the application of tissue recombination (TR), using fetal tissue rescued from *Rb-/-* embryos and propagated in combination with wild type (*Rb+/+*) prostate stromal tissue, has enabled the development of *Rb*-/- prostate (34-36) and mammary grafts (37). In the current study, we describe the isolation and characterization of the *Rb-/-* prostate epithelial cell line, Rb-/-PrE, derived from *Rb-/-* fetal urogenital precursor tissue rescued from embryonic mice (34). To our knowledge, this is the first *in vitro* model to allow for the study of targeted *Rb* deletion on an epithelial population and provides a unique experimental platform with which to investigate the physiological consequences of *Rb* deletion on the regulation of cell cycle, differentiation, cell survival and carcinogenesis.

METHODS

PCR genotyping for Rb*-/- tissues and cell lines*

Heterozygous Rb+/- mice were purchased from Jackson Laboratories (Bar Harbor, ME). To increase litter size and thus the chances of Rb-/- offspring, the heterozygotes were and crossed to CD1 mice. The genetic identity of the offspring was confirmed by PCR genotyping to identify the presence of the neomycin selection cassette that was used to disrupt the Rb gene. The Rb heterozygotes were crossed, fetuses rescued and the prostatic ductal tips were then recombined as described (34). The *Rb* status of tissue grafts was determined by PCR analysis. Control (Jackson Laboratories) and experimental DNA samples were amplified using wild type- and mutant-specific primers, and separated on 2% agarose gels containing ethidium bromide. The protocol for PCR cycling conditions was obtained from the Jackson Laboratory technical support (micetech@jax.org). PCR primers (Jackson Laboratories) used for genotyping tissues and cell lines were as follows: *Rb* knockout allele, forward 5'-AAT TGC GGC CGC ATC TGC ATC TTT ATC GC-3' (oIMR025), reverse 5'-GAA GAA CGA GAT CAG CAG-3' (oIMR027), and *Rb* wild type allele, forward 5'-AAT TGC GGC CGC ATC TGC ATC TTT ATC GC-3' (oIMR025) and reverse 5'-CCC ATG TTC GGT CCC TAG-3' (oIMR026) (10).

Serial Recombination of Rb-/- prostate tissues

Serial tissue recombination was used to assess the ability of the *Rb*-/- epithelial cells to undergo multiple rounds of growth and generate immortalized tissue. A ductal tip of approximately 300µm was micro-dissected from rescued *Rb*-/- prostatic tissue (34), recombined with normal rat urogenital mesenchyme (rUGM) and grafted beneath the renal capsule of an intact male athymic mouse host. After one month of growth, the host was sacrificed and the graft was retrieved. The resultant 40mg of prostatic tissue (38) was again micro-dissected and another 300µm ductal tip

recombined with fresh rUGM and grafted into a new mouse host to produce a "second generation" graft. This recombination protocol, repeated 8 times, resulted in approximately 13 epithelial population doublings for each round of recombination and re-grafting as estimated by the number of epithelial cells from the tissue weight using the Coffey equation $1g=10^9$ cells (39).

Generation of wild-type PrE and Rb-/-PrE Cells

Rb-/- prostate grafts were established in nude mice, then the ductal fragments were recombined with rUGM as described (34). A portion of each excised graft was fixed for histological examination while the rest was utilized to create Rb-/-PrE epithelial cultures. The tissue was minced with a scalpel and forceps and plated onto tissue culture plastic coated with collagen substrate in a minimal volume of medium to allow for attachment of the tissue to the matrix. These tissues were grown in RPMI-1640 (#12-702F BioWhittaker). Culture media was supplemented with ITS (5µg/ml insulin, 5µg/ml transferrin, 5ng/ml selenium, # 40351 Collaborative Research), BPE (10µg/ml bovine pituitary extract, #P1167 Sigma), EGF (10µg/ml Epidermal Growth Factor, #40001 Collaborative Research), Cholera Toxin (1.0µg/ml, #C-8052 Sigma), Amphotericin B (250µg/ml, Fungizone #15295-017 Gibco), Dexamethasone (5µM, #D-2915 Sigma), 200mM L-glutamine (#25030-081 Gibco), and 100 U/ml penicillin G and 100 U/ml streptomycin (#17-602E BioWhittaker). This formulation supports the growth of epithelial cells while retarding the growth of the fibroblast cells. Approximately 10-14 days after plating, the tissue pieces were removed from the cultures and selection was initiated with 200µg/ml G418 (#15-394N BioWhittaker). Once large areas of epithelial cells became established, cells were passaged 1:3 by trypsinization. Between passage 5 and passage10, cultures were gradually switched to a medium containing only 5% FBS, L-glutamine (#25030-081, Gibco), and 100 U/ml

penicillin G and 100 U/ml streptomycin (#15140-148, Gibco) in RPMI-1640 termed "5% FBS growth medium".

Wild type PrE cultures were generated from prostates excised from six-week-old strain-matched male CD1 mice (Harlan Laboratories) following euthanasia with CO_2. Prostate tissues were minced and plated in the defined BPE-containing culture medium described above. These cultures were maintained identical to the Rb-/-PrE described here without the addition of G418. The wild type control cell line, termed PrE, utilized for comparison herein, spontaneously immortalized in culture and was therefore utilized as a control for spontaneous immortalization of mouse prostatic epithelial cultures.

Species Determination of Cells utilizing Hoechst 33258 Staining

Mouse Rb-/-PrE cells were grown on Falcon chamber slides to 70% confluence and fixed with 100% ethanol on ice for 5 minutes before washing with two changes of cold PBS. Fixed cells were then stained with Hoechst 33258 dye (5µg/ml, Sigma #B2883) for 1 minute at room temperature. Following staining, cultures were again washed three times in cold PBS, wet-mounted (Biomeda Corporation) and photographed using a Zeiss Axioskop fluorescent microscope to confirm that the cells were of mouse origin (40).

Long Term Serum Free Growth Analysis

Wild type and Rb-/-PrE (5×10^5) cells were plated into 60mm culture dishes containing 5% FBS growth medium. Three days after plating (termed "Day 0"), culture media was changed to a serum-free media consisting of RPMI-1640 (#12-918F BioWhittaker), 100 U/ml penicillin G and 100 U/ml streptomycin (without phenol red and without L-glutamine). Cultures were fed with the aforementioned serum-free medium every three days and counted at the indicated times, where each time point is the average and standard deviation of triplicate dishes. Viable cell

counts were analyzed by Trypan Blue exclusion. Photographs were taken on a Nikon Diaphot 200 with a Nikon digital camera.

Re-grafting of Rb-/-PrE Cells by Cellular recombination

At passage 21, Rb-/-PrE cells were utilized to generate prostate grafts via cellular recombination. To prepare grafts; 2.5 x 10^5 urogenital mesenchymal cells and 1 x 10^5 Rb-/-PrE cells were combined in a collagen matrix as previously described (41). These grafts were then transplanted beneath the renal capsule of an adult, male nude mouse host (Charles River laboratories) and grown for one month. Host animals were then sacrificed and the grafts were harvested, subjected to fixation and evaluated utilizing immunohistochemical techniques.

Immunohistochemistry

Tissue sections were deparaffinized in Histoclear (National Diagnostic) and hydrated in graded alcoholic solutions and PBS. Endogenous peroxidase activity was blocked with 0.5% hydrogen peroxide in methanol for 30 minutes and washed in PBS prior to staining. Immunocytochemical staining for expression of cytokeratins CK8, CK14 and CK18 in Rb-/-PrE cells was performed as previously described (34). Cells were grown on chamber slides (Falcon) coated with 5μg/ml fibronectin prior to fixation with 100% ethanol for 5 minutes on ice. Cells were then washed with PBS and glucose oxidase substrate was employed in conjunction with the mouse and rabbit Vector Labs staining kits. Staining for the AR and estrogen receptor α (ERα), mDLP and p63 was also repeated with the re-grafted Rb-/-PrE cells (passage 20). Following growth in nude-mouse hosts, the re-grafted tissue was harvested and subjected to the staining procedure as described (34,42).

Western Blot, Antibodies and Protein Analysis

Primary antibodies were obtained as follows: anti-rat E-cadherin (Transduction Laboratories, C20820), anti-Rb (PharMingen, 14001A), anti-p107 (Transduction Laboratories, R27020), anti-p130 (Santa Cruz, SC-318), anti-p21 (PharMingen, 556430), anti-p53 (Oncogene, OP29), anti-AR (Santa Cruz, SC-816), anti-estrogen receptors α and β (Santa Cruz, SC-542 and SC-8974, respectively), anti-cyclin D1 (Santa Cruz, SC-8396), anti-cyclin E1 (Santa Cruz, SC-481), anti-PCNA (Santa Cruz, SC-9857, anti-cyclin A (NeoMarkers, RB-007-P0), anti-actin (Santa Cruz, SC-1615) and high molecular weight pan-cytokeratin (#Z0622 Dako). Horseradish peroxidase-conjugated secondary antibodies were obtained as follows: donkey anti-mouse (Amresco #E974), goat anti- rabbit (BioRad) and donkey anti-goat (BioRad). For protein analysis, cultured cells were lysed on ice in 50 mM Tris, pH 7.5, 120 mM NaCl, 0.5% nonidet P-40, 1mM EGTA and protease inhibitors (40 μM PMSF, 5 μg/ml leupeptin, 50 μg/ml aprotinin, 200μM sodium orthovanidate). Following centrifugation, the supernatants were collected, quantitated using a Bradford microtiter assay, and denatured with a reducing 2X sample loading buffer for 5 minutes at 100°C. All proteins were then separated on Tris/Glycine pre-cast NOVEX gels and analyzed utilizing the ECL detection system (Amersham) as described previously (43).

Growth Kinetics of PrE and Rb-/-PrE Cells

Cultures of PrE and Rb-/- PrE were maintained in RPMI-1640 (BioWhittaker) containing 5% Dextran-coated, Charcoal Stripped (DCC) FBS, termed '5% CCS growth medium' and compared to cultures grown in 5% FBS growth medium. For these experiments, PrE and Rb-/-PrE cells were plated at a density of 5 X 10^5 cells into 100mm culture dishes and viability and cell number was assessed via Trypan Blue (Gibco) exclusion on various days after plating.

Flow Cytometric Evaluations

PrE and Rb-/-PrE (1 x 10^6, passages 15 – 20) were plated into 100mm dishes and analyzed four days later to determine log phase cell cycle profiles. To ascertain growth arrest in confluent cultures, cells were plated at a higher density (2 x 10^6 cells per dish) and retained in culture for a total of 15 days. Serum-containing medium was replaced every three days on the long-term cultures. Cells were harvested by trypsinization, fixed and stained with DAPI (4'6-diamidino-2-phenylindole,dihydrochloride). Prior to examination of cells by flow cytometry, 1 x 10^6 cells were collected by trypsinization, centrifuged and reconstituted with 800µl of PBS (without calcium or magnesium). One drop of an internal trout DNA control (Reiss Enterprise #1007) was added to each sample. Then, 3.5 ml of cold 100% ethanol was added drop-wise while mixing for fixation. Samples were then incubated for one hour on ice prior to centrifugation and re-hydrated with 1 ml of PBS for 15 minutes on ice. Again, all samples were centrifuged and reconstituted with 1.5 ml of DAPI staining buffer (100mM Tris, pH7.4, 150mM NaCl, 1mM $CaCl_2$, 0.5mM $MgCl_2$, and 0.1% Nonidet P-40). A final concentration of 1.0µg/ml DAPI (Molecular Probes #D-1306) was utilized for flow cytometric evaluations. Flow cytometry was carried out at the University of Michigan Flow Cytometry Core facility using Becton Dickinson FACS Vantage SE model 127. Data was acquired to 10^5 events per sample. MultiCycle software (Phoenix Flow Systems, San Diego, CA) was utilized to estimate the percentage of cells in G_1, S and G_2M phases of the cell cycle populations.

Spectral Karyotype (SKY) Analysis and Comparative Genomic Hybridization (CGH):

Metaphase chromosomes from cultures of wild type PrE and Rb-/-PrE were obtained by mitotic shake-off after 1 hour of colcemide (1µg/ml) treatment. Slides were hybridized with SKY kits, prepared from flow-sorted chromosomes and detected 72 hours later as described previously (44). Images of 10-15 metaphase cells were acquired using a DMRXA microscope (Leica,

Wetzlar, Germany) equipped with a custom designed SKY-3 optical filter (Chroma Technology, Brattleboro, VT), a spectral cube and a charge-coupled device camera (Hamamatsu, Bridgewater, NJ). Analysis was performed with SkyView software (Applied Spectral Imaging, Ltd., Migdal Haemek, Israel) as described elsewhere (45). For CGH analysis, DNA was prepared under high salt conditions. Biotin-labeled DNA was derived from PrE and Rb-/-PrE cultures and co-precipitated with digoxigenin-labeled reference DNA obtained from sex- and strain-matched *Rb*+/- and/or *Rb*+/+ mice. DNA was hybridized to sex-matched normal murine (C57) lymphocyte metaphase chromosomes, detected and images acquired with Q-CGH software (Leica Imaging Systems, Cambridge, UK) (46).

RESULTS

Genotype and Phenotype of PrE and Rb-/-PrE Cells. Because the *Rb* gene was disrupted by the insertion of the neomycin resistance cassette (47), the use of cellular recombination (34), employing neomycin-sensitive, wild type rUGM and neomycin-resistant Rb-/-PrE mouse epithelium allowed for the specific selection of Rb-/-PrE from the wild type stroma. Following selection on neomycin for several weeks, PCR genotyping revealed that the Rb-/-PrE cells exhibited only the larger 420 bp mutant PCR product compared to the 400bp wild-type PCR product or the mixed PCR products of the heterozygous control cells (figure 1A). Western analysis of Rb-/-PrE cells revealed complete loss of pRb protein expression while maintaining E-cadherin (epithelial-cadherin) protein expression (figure 1B), confirming the *Rb-/-* genotype and epithelial lineage of the Rb-/-PrE cells. Rb-/-PrE cultures growing in 5% FBS growth medium were photographed at sub-confluent and confluent densities utilizing phase-contrast microscopy (figure 1C). Staining Rb-/-PrE cells with Hoechst 33258 dye revealed homogeneous, punctate nuclear patterns characteristic of mouse cells while control rat epithelial cells exhibited a non-punctate staining pattern, confirming that Rb-/-PrE cells were not derived from rat tissues (figure1C).

Analysis of Rb-/-PrE survival and growth in the absence of serum. Rb appears to play a paradoxical role in the regulation of cell survival, as evidence has emerged supporting both pro- and anti-apoptotic functions of the protein (4). Wild type PrE and Rb-/-PrE cells cultured beyond passage 8 are maintained in media supplemented with 5% FBS. We wanted to determine whether Rb-/-PrE cells could continue to proliferate in the absence of serum containing growth factors and determine if the loss of pRb would compromise survival. Viable cell counts of PrE

and Rb-/-PrE cultures were documented under serum-free conditions (figure 2A). Rb-/-PrE cells remained viable and continued to proliferate for more than 50 days in serum-free media, whereas the wild type PrE cells ceased to proliferate and exhibited a marked loss in viability. These results suggest that the Rb-/-PrE cultures can circumvent cell death programs in the absence of growth factors.

We rationalized that the loss of Rb would allow cells to override growth-restraining or apoptotic mechanisms that may result in immortalization. We could demonstrate that the Rb-/-PrE epithelial cells did not senesce and continued to proliferate for more than 120 passages (figure 2B). These results are in contrast to previous studies of *Rb*-/- mouse embryonic fibroblasts in which these cells senesced at early passage (19,48). Even though Rb-/-PrE cells are immortal in culture, spontaneous immortalization of murine cells has been reported (49), and we have observed the spontaneous immortalization of approximately half of our wildtype PrE cultures (data not shown). To determine that the immortalization of Rb-/-PrE cells resulted from artifactual effects of cell culturing or was a specific outcome of Rb disruption, we examined the immortalization of Rb-/-PrE cells in recombinant tissue grafts *in vivo*. PrE and Rb-/-PrE grafts were subjected to multiple rounds of serial tissue recombination with rUGM in male athymic-mouse hosts. Serial regrafting was repeated for up to seven additional passages *in vivo*, for a total of eight *in vivo* passages. Each *in vivo* passage (to expand epithelial cell growth) represents approximately 13 population doublings. The wild type grafts only proliferated and survived through three rounds of serial regrafting. In contrast, the Rb-/-PrE grafts survived eight rounds of recombination *in vivo*, and were still viable at the termination of the experiment (figure 2C).

The loss of Rb does not influence prostatic histodifferentiation and morphogenesis *in vitro*

and *in vivo*. *Rb* is believed to play an active role in tissue development by regulating a post-mitotic state required for cellular differentiation, including androgen-mediated differentiation of prostate epithelium, reviewed in (50). Morphologic examination and E-cadherin expression in figure 1 confirmed the epithelial lineage of the mouse Rb-/-PrE cells. To examine more closely the state of Rb-/-PrE prostatic differentiation in culture cells, we examined a number of prostatic and epithelial markers. Cytokeratin expression was assessed in Rb-/-PrE cells revealing low expression of the basal epithelial marker, cytokeratin 14, and high expression of the luminal epithelial marker, cytokeratin 18 (figure 3 A, B respectively), indicating a mixed epithelial population dominated by a luminal phenotype. Western blot analysis of Rb-/-PrE cultures at early and later passage also revealed strong androgen receptor (AR) and estrogen receptor beta (ER β) expression (figure 3C) where the estrogen receptor α immuno-reactivity was negative (data not shown). These results demonstrated that the Rb-/-PrE cells continued to express prostate-specific markers even after many passages in culture.

To determine if Rb-/-PrE cells could recapitulate prostate histodifferentiation and morphogenesis *in vivo*, the Rb-/-PrE (passage 20) and wild type PrE (passage 20) were recombined with rUGM, and grafted into intact male athymic host mice. Hematoxylin and eosin (H&E) staining revealed that the wild type rUGM+PrE grafts (figure 4 A) and the rUGM+Rb-/-PrE grafts (figure 4B) were indistinguishable. Both grafts exhibited normal prostate glandular morphology and stained positively for AR and for the murine, prostate-specific dorsal lateral protein marker (mDLP), confirming the murine prostate lineage of this graft (figure 4C, D). It has been previously reported that, p63, a homologue of p53, is expressed in basal epithelium of glandular tissue, such as the prostate gland, and that p63 is required for prostatic development (42). Staining with a p63 antibody revealed strong staining in a population of basal cells just

beneath the luminal component in both wild type and Rb-/- grafts (figure 4E, F). These findings confirm the ability of Rb-/-PrE cells to recapitulate normal prostatic histo-differentiation and morphogenesis *in vivo.*

Rb-/-PrE cells retain intact p107/p130 and p53/p21 pathways. Beyond the established role of pRb in cell cycle arrest, the involvement of p107 and p130 in the inhibition of cell growth has also been documented in several cell types (18). In normal cells the levels of p130 and p107 change dramatically during the cell cycle. When cells are engaged in cycle and moving through S phase, the expression of p130 is low, however, when cells are forced to exit the cell cycle by serum withdrawal or contact inhibition, p130 protein accumulates rapidly (13,15). The expression of p107 is modulated in an opposing manner to p130. P107 is present at high levels in cycling cells, and like pRb is hyperphosphorylated, however, when cells exit cycle in response to serum withdrawal or contact inhibition, p107 is rapidly dephosphorylated and protein levels decrease. To determine if the immortalized, serum-independent phenotype of Rb-/-PrE cells resulted exclusively from *Rb* loss and not from ancillary loss of p107 or p130, we examined the expression of these proteins in control PrE and Rb-/-PrE cells in either sub-confluent, serum free or high-density culture conditions. In sub-confluent cultures, the hyper- and hypophosphorylated forms of p107 were detected in the control PrE and Rb-/-PrE cells. Western blot analysis of both PrE and Rb-/-PrE cells revealed that p107 was dephosphorylated and protein levels were dramatically reduced in serum-free and high-density cultures (figure 5A). From the same lysates, levels of p130 were slightly elevated in untreated PrE cells compared to Rb-/-PrE, but accumulated to the same extent in both cell lines under serum-free and high-density culture

conditions (figure 5B). These results demonstrated that p107 and p130 respond normally to G_1 growth arrest signals in Rb-/-PrE cells and wildtype PrE control cultures.

Physiologic exit from cell cycle and the induction of growth arrest have been linked to p53 and p53-dependent cell cycle inhibitors $p19^{Arf}$ and $p21^{Cip1}$ (51). Cell cycle exit in response to non-physiologic signals such as treatment with ionizing radiation and DNA intercalating agents have also been shown to be regulated by the p53-dependent activation of p21. To confirm that the immortalizing effects observed in Rb-/-PrE cells was a direct result of *Rb* loss and not a result of ancillary loss of p53 and/or p21, the expression and functionality of these proteins in Rb-/-PrE cells was examined. Western blot analysis of Rb-/-PrE cells demonstrated that induction of p53 protein was comparable to those observed in wild type cells following UV-irradiation (figure 5C). Levels of p21 were also induced following UV irradiation in both Rb-/-PrE and wild type cells (figure 5D). These results suggest that the p53 pathway is functional in the Rb-/-PrE cultures.

Growth kinetics of PrE and Rb-/-PrE cultures. To compare growth characteristics of PrE to Rb-/-PrE cells, proliferation studies were performed on passages 20-22 of these two cell lines. At the indicated times, the cells were trypsinized, counted and the viability was assessed by Trypan Blue exclusion assay. Figure 6 is a representative experiment demonstrating PrE and Rb-/-PrE growth kinetics. The results demonstrate that the 5% FBS growth medium supported the growth of both cell lines. Additionally, there was a two-fold enhanced proliferation rate of the Rb-/-PrE cells over the control PrE cells. To compare the growth kinetics in the absence of hormones and steroids, we performed this same experiment with cells cultured in dextran-coated, charcoal-stripped 5% serum growth medium (5% DCC). We found that under this culture condition, both

cell lines grow equally well in the presence or absence of steroids.

Analysis of cell cycle re-entry in serum-free synchronized PrE and Rb-/-PrE cells. We next wanted to investigate the mechanism(s) that may be responsible for the increased growth kinetics of the Rb-/-PrE cells. The expression levels of cell cycle regulatory proteins were assessed in synchronized wildtype and Rb-/-PrE cells as these cells re-entered cycle following serum starvation. At the indicated times, the cells were harvested and analyzed for protein expression of cyclin D1, cyclin E1, PNCA and actin. PrE cells exhibit slightly higher levels of cyclin D1 expression compared to the Rb-/-PrE cells, however cyclin D1 increased in both lines as they reenter the cell cycle (figure 7). In contrast, expression of cyclin E1 and PCNA are significantly elevated in Rb-/-PrE compared to the wild type control. Both PCNA and cyclin E1 have been found in complex with E2F transcription factors at the G_1/S phase border of the cell cycle and are believed to play a critical role in the activation of several S phase-specific proteins (52,53). Therefore, the loss of *Rb* and liberation of E2F1 likely promotes the expression of E2F target genes, such as cyclin E1 and PCNA, that in turn drive the cells into DNA synthesis, resulting in the enhanced growth kinetics profile, as seen in the Rb-/-PrE cells.

Rb-/-PrE cells have an increased DNA ploidy. To better understand the functional consequences of *Rb* loss on cell cycle regulation in prostate epithelial cells, we evaluated the potential of these cultures to undergo G_1 arrest under high-density culture conditions in the presence of serum growth factors. PrE and Rb-/-PrE cultures were grown in 5% FBS and analyzed at sub-confluent and high-density culture conditions by flow cytometry. At sub-confluent culture conditions, there was no significant difference in the distribution of cells in the

various phases of the cell cycle between PrE and Rb-/-PrE cells. When PrE and Rb-/-PrE cultures were maintained at high density (15 days) in 5% FBS growth medium, some differences were noted in the DNA ploidy (figure 8 C, D). The was an increase in DNA content of Rb-/-PrE cells compared to wild type PrE cells as indicated by the increases of the mean G_1 value of 124 units vs. 194 units in the Rb-/-PrE cells. However, in high-density cultures, the distribution of cells in G_1 is similar, with PrE and Rb-/- exhibiting 61% and 70% G_1 respectively. In multiple experiments, we noted differences in the distribution of cells in S phase, where the Rb-/-PrE cultures had approximately 2-fold higher S phase content than wild type PrE cells. Therefore the data shown in figure 8 revealed that while both PrE and Rb-/-PrE cells have similar G_1 distribution, the Rb-/-PrE cells have increased DNA content (ploidy) as compared to wild type.

Karyotyping of Rb-/-PrE cell line. To determine the extent of chromosomal abnormalities that may have resulted following *Rb* loss, chromosomal integrity of the Rb-/-PrE cells was analyzed by spectral karyotyping (SKY). As shown (figure 9A), metaphase chromosomes from two cell lines representing an early passage (passage 14) and a later passage (passage 25) were obtained by mitotic shake-off and subjected to SKY analysis. Both passages were hypertriploid with gains corresponding to 4-6 copies of chromosome 19 in all cells and a recurring loss of chromosome 4 (2 copies of chromosome 4 in 60% of cells). The Rb-/-PrE cells also revealed recurring but lower level gains of chromosome 15, as well as a rare translocation involving chromosomes Y and 17. The ISCN karyotype of the passage 14 Rb-/-PrE cells showed: 59-70 XY, +X [10], +Y[9], der(Y)t(Y;17)(B1;D1)[2], -4[6], +5[5], +8[3], +9[5], +10 [5], +11[4], +15[10], +16[4], +17[3], +18[3], +19x2 [10] [cp10]. The ISCN karyotype of 10 cells of the passage 25 Rb-/-PrE was similarly hypertriploid and had a ISCN karyotype of: 61-74 XY, +X[8],+Y [6], -4[6], +5[5], -

6[3], +7[2], +8[5], +9[6], +10[8], -11[6], +12 [5], +13 [4], +14 [3], -15[3], +15[3], +16[4], +19x2 [10] [cp10]. No cells were karyotypically identical and each cell exhibited an average of 8 chromosomal gains or losses from a modal number of 3.

To assess the above changes on the genomic DNA level, comparative genomic hybridization (CGH) was performed with DNA extracted from Rb-/-PrE cell lines at passages 10, 20, and 40 and control DNA extracted from strain-matched wild type mouse DNA. Results showed that all three Rb-/-PrE DNA samples from passages 10, 20 and 40 shared loss of chromosome 4 and gains of chromosome 19, although by passage 40 there was significant amplification of chromosome 19 as well as one copy gains of chromosomes 6, 11 and 15. These data strongly suggest that the homozygous loss of *Rb* resulted in chromosomal changes including the loss of mouse chromosome 4 and significant gains of chromosome 19 over the wild type control (figure 9B and data not shown).

DISCUSSION

Until now, the lethal nature of the *Rb* knockout precluded the establishment of *Rb-/-* epithelial cell lines, with which definitive experiments to investigate physiological roles for *Rb* in specific epithelial populations could be performed. The current study describes the successful establishment of an *Rb-/-* prostate epithelial cell line that was rescued from fetal urogenital precursor tissue. The resultant cell line, termed Rb-/-PrE, was utilized for the physiologic examination of *Rb* deletion in a specific epithelial population.

Historically, the use of transforming oncogenes, such as E1a, E6/E7 and large T antigen, have been useful to address *Rb* function, however these reagents do not exclusively target *Rb* and

promote such genomic instability that experimental interpretation are difficult. The chromosomal imbalances directly influenced by viral oncogenes have been identified as predominantly random genetic events. (31-33). One of the central objectives of this study was to delineate and characterize the physiological function of pRb in a prostate epithelial population, if possible, with minimal complications of genetic instability inherent in tumor cells and cells transformed with viral oncogenes. Therefore, the state of chromosomal integrity was essential in the characterization of the Rb-/-PrE line.

SKY analysis revealed that the deletion of *Rb* in prostate epithelium gave rise to aberrations that are consistent with immortalization. Aneuploidy in the Rb-/-PrE cells characterized by the loss of chromosome 4 and gains of chromosome 19 were the prominent, recurring events. When these cells were analyzed at passages 14 and 25, Rb-/-PrE cells were hypertriploid with 59-70 and 61-74 chromosomes per cell respectively compared to a hyperdiploid state of 42-43 chromosomes per cell in the PrE wildtype controls at passage 14 (data not shown) where normal mouse cells have 40 chromosomes. At passage 72 the Rb-/-PrE cells were hypertriploid to hexaploid exhibiting 61-136 chromosomes. Our control, wildtype PrE cell line, which had spontaneously immortalized in culture, also demonstrated loss of chromosome 4 and one copy gains of chromosomes 2, 11, 18, and 19. The copy number of chromosome 19 in the Rb-/-PrE cells increased with passage number up to 12 copies of chromosome 19 detected at passage 72. Rb-/-PrE cells also demonstrated recurring but lower level gains of chromosomes 5, 6, 11, 15 and 18 at passages 20-72. In addition to these aberrations, the early passage of Rb-/-PrE cells also had a rare (i.e.2 of 10 cells) structural aberration involving chromosomes Y and 17.

The gain of chromosome19 was more prominent in the Rb-/-PrE cells than in the wild type PrE cells (12 copies vs.1) and may reflect a more specific outcome of *Rb* disruption. Trisomy 19 has been implicated in early tumorigenesis in murine hepatocellular carcinoma and disorders of the murine central nervous system (54,55). Furthermore, gains of hamster chromosome 3q, which shares homology with mouse chromosome 19, have also been associated with immortalization *in vitro* (56,57). These data suggest that the high level gain of chromosome 19 may convey an early selective advantage on the Rb-/-PrE cells due to an increased copy number of growth-related genes and/or true oncogenes that reside on chromosome 19.

The loss of chromosome 4 is a recurring event in both the wild type PrE cells and Rb-/-PrE cells and, at a threshold level, may result in part from unrelated events due to culturing. But, evidence does exist that suggests a selective pressure may, in part, be caused by this *Rb* null genotype. Although the Rb-/-PrE cells are not completely immune to genetic alterations, the chromosomal changes described here are minimal and reflect a specific increase in chromosome 19. The Rb-/-PrE cells are not prone to the more frequent genetic translocations attained in cells associated with p53 mutation tumorigenesis, viral-oncogenic transformation. The finding that the Rb-/-PrE line, while susceptible to chromosomal gain, does not exhibit chromosomal rearrangement or translocation due to an intact p53 repair mechanism.

Numerous studies have suggested that pRb plays an essential role in embryonic development (9-11), and the deletion of *Rb* in a variety of models resulted in marked abnormalities in the differentiation of specific cell types (5-7). In this study, we have demonstrated that despite the lack pRb protein expression, Rb-/-PrE cells continue to express markers of terminally differentiated prostatic epithelium and that these cells are fully capable of recapitulating normal prostatic morphogenesis *in vivo*, complete with expression of prostate-

specific secretory proteins. It has been suggested that cellular differentiation can be divided into three general steps: cell cycle exit, protection from apoptosis, and tissue-specific gene expression (58). Our findings suggest that the loss of Rb does override the ability of Rb-/-PrE cells to growth arrest. A role for Rb disruption in immortalization is more strongly suggested by the *in vivo* experiments demonstrating that only the Rb-/-PrE grafts and not wild type grafts were immortal. The Rb-/-PrE cells were also able to survive in serum-free media, a condition that eventually induces cell death in the wild type controls. Lastly, we found that *Rb* loss does not effect the ability of prostate epithelium to undergo normal prostatic histodifferentiation and recapitulate prostate morphogenesis. This is in agreement with another study demonstrating that the loss of Rb did not adversely affect the normal development of murine mammary gland (37).

The *Rb* gene product regulates the transition between G_1 and S phases in the cell cycle and functions in transducing growth-inhibitory signals that arrest cells in $G_{1.}$ Deletion of *Rb* in a variety of cancer cell types has been associated with a deregulated cell cycle and endoreduplication (59). When PrE and Rb-/-PrE cells were analyzed for differences in expression of cell cycle regulatory proteins, enhanced expression of cyclin E1 in conjunction with increased PCNA levels were noted in the Rb-/-PrE cells, whereas cyclin D1 levels were reduced. Increased expression of cyclin E and PCNA in the Rb-/-PrE cells were likely due to the liberation of E2F and subsequent activation of transcription. The finding, that cyclin D1 was repressed in the Rb-/-PrE cultures might be explained by an independent transcriptional mechanism by which E2F-1 and SP1 cooperate to repress cyclin D1 transcription at specific sites in the cyclin D1 promoter (60). The observation that E2F may regulate such opposing outcomes of different cell cycle regulatory targets suggests a clear dissociation of these two pathways in prostate epithelium. The Rb-/-PrE cells are more active in DNA synthesis and this may be

attributed to the increased cell growth kinetics and loss of growth arrest potential of these cells. These results support the hypothesis that; the loss of *Rb* does result in a more proliferative and aneuploid phenotype and contribute to alterations in cell cycle regulatory proteins possibly through a constitutively active E2F1. A downstream effect of this enhanced proliferative activity may result in the compression of the G_2/M phase as noted in the Rb-/-PrE cultures at high density. This experiment provides an excellent example of the regulatory control provided by pRb at the G_1/S border where, in the absence of pRb, E2F is free to activate genes such as cyclin E1 and PCNA that drive DNA synthesis. These findings suggest that the loss of *Rb* on a specific epithelial population may circumvent growth inhibitory constraints that support the immortalized phenotype and promote epithelial survival in the absence of peptide growth factors.

Cellular senescence has been associated with a reduction in telomere length. This hypothesis was supported by studies demonstrating a direct link between limited cell division and progressive telomeric shortening**.** It was also postulated that maintenance of telomere length by telomerase might override senescence. Such a causal role for telomerase in cellular senescence has been demonstrated by transfection of the human telomerase reverse transcriptase (hTERT) cDNA into normal cells resulting in their ability to bypass senescence and prolong life span *in vitro* (61). We found that telomerase activity was elevated in both Rb-/-PrE, but because telomerase activity was also elevated in the spontaneously immortalized control wildtype PrE cells, it is impossible to conclude that there is a specific regulatory role for Rb in telomerase expression. These results do suggest, however, that telomerase activity may be important in the immortalization of mouse epithelial cells.

The similarities and differences between pRb, p130 and p107 are apparent in mice carrying single or compound knockouts of the corresponding genes. When the *Rb* gene is deleted

through homologous recombination, embryos die at 13 days of gestation from defective development of erythroid and neuronal tissues (9-11). In stark contrast, targeted disruption of either p107 or p130 is not lethal and does not result in an obvious phenotype (20,62). Recent studies have demonstrated that mouse embryonic fibroblasts (MEFs) harboring a triple knockout of pRb, p107 and p130, are resistant to G_1 arrest signals and do not undergo senescence in culture (19,48). These cells also exhibit some features of transformed cells, such as focal proliferation on monolayers and anchorage-independent growth, however, individual mutants do not undergo transformation. As with the *Rb-/-* fibroblasts, *Rb-/-* prostate epithelial cells do not exhibit characteristics of transformation. While mutation of individual Rb family members in MEFs resulted in minor alterations in both cell cycle regulation and DNA damage response, these cells still remained sensitive to G_1 arrest signals and subsequently entered into senescence. In general, the cell cycle studies of Rb-/-PrE epithelial cells supported those findings in MEF cells, in that Rb deletion resulted in only minor changes in cell cycle regulation. Taken together, these results suggest that cell cycle regulation and cellular transformation of *Rb-/-* MEFs and Rb-/-PrEs are not attained by a single mutation of the *Rb* gene and is likely influenced by the simultaneous disruption of all three pocket protein family members. In contrast to the findings in *Rb-/-* MEFs, our results suggested that the loss of Rb does support the immortalization of prostate epithelium, particularly *in vivo*.

The RB gene encodes a key regulatory component of the cell cycle that is frequently disrupted in many human cancers, including adenocarcinoma of the prostate gland, reviewed in (50). In a recently published model of mouse prostate cancer, the use of Rb-/-PrE prostatic tissue and its response to hormonal carcinogenesis were described (34). In that study, *Rb-/-* prostatic tissue was highly susceptible to hormone-induced malignant transformation. This model has

drawn much interest due to the recapitulation of several key features of human prostate cancer, namely in its progression from dysplasia to carcinoma accompanied by the loss of the basal epithelium. The role of pRb in human neoplasia, including prostate carcinoma, has been the subject of rigorous investigation for a number of years; however, the specific function of pRb in the etiology of prostate tumorigenesis has yet to be determined.

If *Rb* inactivation has a role in epithelial transformation, the question arises: Does the inactivation of *Rb* influence an immortalized phenotype by overriding growth inhibitory or apoptotic mechanisms *or* does the inactivation of *Rb* result in alterations that lead to transformation? We hypothesized that the specific loss of *Rb* in an epithelial population would disrupt the G_1 restriction point, allowing these cells to bypass senescence. Our data demonstrated that Rb-/-PrE were immortal *in vitro* and *in vivo*, but were not transformed. The degree of cellular transformation was determined by the inability of Rb-/-PrE cells to form colonies in soft agar, invade through biological membranes or to induce tumors when injected sub-cutaneously into nude mice, compared to transformed prostate cancer cells (data not shown). Thus, the loss of *Rb* may be an event that is required for the immortalization of prostate epithelial cells as other growth-inhibitory pathways, such as p53/p21 and p107/p130 appear intact. It remains to be determined what additional alterations are required on the *Rb-/-* background to promote full transformation of these cells. Identifying these events in the context of *Rb* loss would be invaluable in elucidating the sequence of molecular events leading to epithelial transformation.

ACKNOWLEDGMENTS

The authors wish to acknowledge Donna L. LiVant, Sonja Markwart and Le Way Bao for their expertise and experimental assistance in the evaluation of cellular migration. Additionally, we

wish to thank Ann Marie DesLauriers and Karen A. Peterson for their assistance in the flow cytometry core at the University of Michigan.

GRANTS AND FUNDING

Supported by the National Cancer Institute Specialized Programs of Research Excellence (SPORE) in Prostate Cancer Grants P50 CA69568 and DK56137 at the University of Michigan. This work was supported in part by the UM-Comprehensive Cancer Center NIH F005192, the UM-Rheumatic Diseases Core Center NIH F005952, and the UM-BRCF Core Flow Cytometry facility. Funding was also supported in part from CA96403 at the University of Vanderbilt. Additionally, the animals and recombination technology was funded by DK47517, CA64872, CA59831, CA84294, and by CA89520 at the University of California, San Francisco.

REFERENCES

1. Chen, P. L., Scully, P., Shew, J. Y., Wang, J. Y., and Lee, W. H. (1989) *Cell* **58**, 1193-1198.
2. Hinds, P. W., Mittnacht, S., Dulic, V., Arnold, A., Reed, S. I., and Weinberg, R. A. (1992) *Cell* **70**, 993-1006.
3. Brehm, A., and Kouzarides, T. (1999) *Trends Biochem Sci* **24**, 142-145.
4. Zheng, L., and Lee, W. H. (2001) *Exp Cell Res* **264**, 2-18.
5. Lipinski, M. M., and Jacks, T. (1999) *Oncogene* **18**, 7873-7882.
6. Thomas, D. M., Carty, S. A., Piscopo, D. M., Lee, J. S., Wang, W. F., Forrester, W. C., and Hinds, P. W. (2001) *Mol Cell* **8**, 303-316.
7. Wagner, M., Miles, K., and Siddiqui, M. A. (2001) *Dev Dyn* **220**, 198-211.
8. Day, M. L., Foster, R. G., Day, K. C., Zhao, X., Humphrey, P., Swanson, P., Postigo, A. A., Zhang, S. H., and Dean, D. C. (1997) *Journal of Biological Chemistry* **272**, 8125-8128
9. Clarke, A. R., Maandag, E. R., van Roon, M., van der Lugt, N. M., van der Valk, M., Hooper, M. L., Berns, A., and te Riele, H. (1992) *Nature* **359**, 328-330
10. Jacks, T., Fazeli, A., Schmitt, E. M., Bronson, R. T., Goodell, M. A., and Weinberg, R. A. (1992) *Nature* **359**, 295-300
11. Lee, E. Y., Chang, C. Y., Hu, N., Wang, Y. C., Lai, C. C., Herrup, K., Lee, W. H., and Bradley, A. (1992) *Nature* **359**, 288-294.
12. Chellappan, S. P., Hiebert, S., Mudryj, M., Horowitz, J. M., and Nevins, J. R. (1991) *Cell* **65**, 1053-1061.

13. Dyson, N. (1998) *Genes Dev* **12**, 2245-2262.
14. Nevins, J. R. (1998) *Cell Growth Differ* **9**, 585-593.
15. Mulligan, G., and Jacks, T. (1998) *Trends Genet* **14**, 223-229.
16. Weinberg, R. A. (1995) *Cell* **81**, 323-330.
17. Jiang, Z., Zacksenhaus, E., Gallie, B. L., and Phillips, R. A. (1997) *Oncogene* **14**, 1789-1797.
18. Zhu, L., van den Heuvel, S., Helin, K., Fattaey, A., Ewen, M., Livingston, D., Dyson, N., and Harlow, E. (1993) *Genes Dev* **7**, 1111-1125.
19. Dannenberg, J. H., van Rossum, A., Schuijff, L., and te Riele, H. (2000) *Genes Dev* **14**, 3051-3064.
20. Lee, M. H., Williams, B. O., Mulligan, G., Mukai, S., Bronson, R. T., Dyson, N., Harlow, E., and Jacks, T. (1996) *Genes Dev* **10**, 1621-1632.
21. Lassar, A. B., Skapek, S. X., and Novitch, B. (1994) *Curr Opin Cell Biol* **6**, 788-794.
22. Singh, G., Lakkis, C. L., Laucirica, R., and Epner, D. E. (1999) *J Cell Physiol* **180**, 431-438.
23. Knudsen, K. E., Arden, K. C., and Cavenee, W. K. (1998) *J Biol Chem* **273**, 20213-20222.
24. Chen, Y., Robles, A. I., Martinez, L. A., Liu, F., Gimenez-Conti, I. B., and Conti, C. J. (1996) *Cell Growth Differ* **7**, 1571-1578.
25. Yeh, S., Miyamoto, H., Nishimura, K., Kang, H., Ludlow, J., Hsiao, P., Wang, C., Su, C., and Chang, C. (1998) *Biochem Biophys Res Commun* **248**, 361-367.
26. Blagosklonny, M. V., Prabhu, N. S., and El-Deiry, W. S. (1997) *Cancer Research* **57**, 320-325
27. Bookstein, R., Shew, J. Y., Chen, P. L., Scully, P., and Lee, W. H. (1990) *Science* **247**, 712-715.
28. DeCaprio, J. A., Ludlow, J. W., Figge, J., Shew, J. Y., Huang, C. M., Lee, W. H., Marsilio, E., Paucha, E., and Livingston, D. M. (1988) *Cell* **54**, 275-283.
29. Ozer, H. L. (2000) *Prog Mol Subcell Biol* **24**, 121-153
30. Zwerschke, W., and Jansen-Durr, P. (2000) *Adv Cancer Res* **78**, 1-29
31. Tsao, S. W., Wong, N., Wang, X., Liu, Y., Wan, T. S., Fung, L. F., Lancaster, W. D., Gregoire, L., and Wong, Y. C. (2001) *Cancer Genet Cytogenet* **130**, 141-149.
32. Cottage, A., Dowen, S., Roberts, I., Pett, M., Coleman, N., and Stanley, M. (2001) *Genes Chromosomes Cancer* **30**, 72-79.
33. Wan, T. S., Chan, L. C., Ngan, H. Y., and Tsao, S. W. (1997) *Cancer Genet Cytogenet* **95**, 166-172.
34. Wang, Y., Hayward, S. W., Donjacour, A. A., Young, P., Jacks, T., Sage, J., Dahiya, R., Cardiff, R. D., Day, M. L., and Cunha, G. R. (2000) *Cancer Res* **60**, 6008-6017.
35. Phillips, J. L., Hayward, S. W., Wang, Y., Vasselli, J., Pavlovich, C., Padilla-Nash, H., Pezullo, J. R., Ghadimi, B. M., Grossfeld, G. D., Rivera, A., Linehan, W. M., Cunha, G. R., and Ried, T. (2001) *Cancer Res* **61**, 8143-8149.
36. Hayward, S. W., Wang, Y., Cao, M., Hom, Y. K., Zhang, B., Grossfeld, G. D., Sudilovsky, D., and Cunha, G. R. (2001) *Cancer Res* **61**, 8135-8142.
37. Robinson, G. W., Wagner, K. U., and Hennighausen, L. (2001) *Oncogene* **20**, 7115-7119.
38. Norman, J. T., Cunha, G. R., and Sugimura, Y. (1986) *Prostate* **8**, 209-220
39. DeKlerk, D. P., and Coffey, D. S. (1978) *Invest Urol* **16**, 240-245.

40. Cunha, G. R., and Vanderslice, K. D. (1984) *Stain Technol* **59**, 7-12.
41. Hayward, S. W., Haughney, P. C., Lopes, E. S., Danielpour, D., and Cunha, G. R. (1999) *Prostate* **39**, 205-212.
42. Signoretti, S., Waltregny, D., Dilks, J., Isaac, B., Lin, D., Garraway, L., Yang, A., Montironi, R., McKeon, F., and Loda, M. (2000) *Am J Pathol* **157**, 1769-1775.
43. Zhao, X., Gschwend, J. E., Powell, C. T., Foster, R. G., Day, K. C., and Day, M. L. (1997) *Journal of Biological Chemistry* **272**, 22751-22757
44. Difilippantonio, M. J., Zhu, J., Chen, H. T., Meffre, E., Nussenzweig, M. C., Max, E. E., Ried, T., and Nussenzweig, A. (2000) *Nature* **404**, 510-514.
45. Liyanage, M., Coleman, A., du Manoir, S., Veldman, T., McCormack, S., Dickson, R. B., Barlow, C., Wynshaw-Boris, A., Janz, S., Wienberg, J., Ferguson-Smith, M. A., Schrock, E., and Ried, T. (1996) *Nat Genet* **14**, 312-315.
46. Weaver, Z. A., McCormack, S. J., Liyanage, M., du Manoir, S., Coleman, A., Schrock, E., Dickson, R. B., and Ried, T. (1999) *Genes Chromosomes Cancer* **25**, 251-260.
47. Williams, B. O., Schmitt, E. M., Remington, L., Bronson, R. T., Albert, D. M., Weinberg, R. A., and Jacks, T. (1994) *EMBO Journal* **13**, 4251-4259
48. Sage, J., Mulligan, G. J., Attardi, L. D., Miller, A., Chen, S., Williams, B., Theodorou, E., and Jacks, T. (2000) *Genes Dev* **14**, 3037-3050.
49. Kubbies, M., Friedl, R., Bettecken, T., and Hoehn, H. (1986) *Cytometry* **7**, 551-557.
50. Abate-Shen, C., and Shen, M. M. (2000) *Genes Dev* **14**, 2410-2434.
51. Weber, J. D., Jeffers, J. R., Rehg, J. E., Randle, D. H., Lozano, G., Roussel, M. F., Sherr, C. J., and Zambetti, G. P. (2000) *Genes Dev* **14**, 2358-2365.
52. Harbour, J. W., and Dean, D. C. (2001) *Curr Top Microbiol Immunol* **254**, 137-144
53. DeGregori, J., Leone, G., Ohtani, K., Miron, A., and Nevins, J. R. (1995) *Genes Dev* **9**, 2873-2887.
54. Danielsen, H. E., Brogger, A., and Reith, A. (1991) *Carcinogenesis* **12**, 1777-1780.
55. Lorke, D. E. (1994) *Acta Anat* **150**, 159-169
56. Kraemer, P. M., Ray, F. A., Bartholdi, M. F., and Cram, L. S. (1987) *Cancer Genet Cytogenet* **27**, 273-287.
57. Yang, F., O'Brien, P. C., and Ferguson-Smith, M. A. (2000) *Chromosome Res* **8**, 219-227
58. Yee, A. S., Shih, H. H., and Tevosian, S. G. (1998) *Front Biosci* **3**, D532-547.
59. Niculescu, A. B., 3rd, Chen, X., Smeets, M., Hengst, L., Prives, C., and Reed, S. I. (1998) *Mol Cell Biol* **18**, 629-643.
60. Watanabe, G., Albanese, C., Lee, R. J., Reutens, A., Vairo, G., Henglein, B., and Pestell, R. G. (1998) *Mol Cell Biol* **18**, 3212-3222.
61. Bodnar, A. G., Ouellette, M., Frolkis, M., Holt, S. E., Chiu, C. P., Morin, G. B., Harley, C. B., Shay, J. W., Lichtsteiner, S., and Wright, W. E. (1998) *Science* **279**, 349-352.
62. Cobrinik, D., Dowdy, S. F., Hinds, P. W., Mittnacht, S., and Weinberg, R. A. (1992) *Trends Biochem Sci* **17**, 312-315.

FIGURE LEGENDS

Figure 1. Verification of Rb-/-PrE genotype and murine epithelial histology. (A) Primer sets 025-026 (*Rb*+/+) and 025-027 (*Rb*-/-) amplified only wild-type (*Rb*+/+) alleles (400bp) from wild-type mouse-tail DNA (lane 1) and wild-type PrE cells (lane 2). The same primer sets amplified wild type and mutant alleles from heterozygous control cells (lanes 3 and 4). Only the mutant allele (420bp) was amplified with these primer sets from passage 4 and passage 10 Rb-/-PrE cells (lanes 5 and 6). (B) Rb-/-PrE cells lack the 110-kDa pRb protein but strongly express E-cadherin, which also serves as a loading control. (C) Phase-contrast microscopy of Rb-/-PrE cells at sub-confluent (1) and confluent (2) densities. The punctate nuclear staining pattern of the Hoechst 33258 stain is evident in mouse Rb-/-PrE cells (3), while absent in the Dunning rat control epithelial cells (4).

Figure 2. Rb-/-PrE cells are viable in the absence of serum and are immortal *in vitro* and *in vivo*. (A) Wild type PrE and Rb-/-PrE cells were grown under serum-free conditions and viable cells were counted at the indicated times. Results are reported as the average percent relative viability from three independent experiments. (B) The number of passages for which the Rb-/-PrE cells have been cultured by trypsinization in serum-containing media. (C) Wild type PrE cells and Rb-/-PrE cells were utilized for tissue recombination and the number of viable serial passages of the grafts obtained is indicated (C).

Figure 3. Rb-/-PrE cells retain prostate-specific markers. Phase-contrast microscopy of sub-confluent Rb-/-PrE cultures immuno-stained with antibodies against (A) cytokeratin 14 and (B)

cytokeratin 18. (C) PrE and Rb-/-PrE cellular lysates were resolved by SDS-PAGE and probed with anti-AR and anti-ER β antibodies at various passages.

Figure 4. Rb-/-PrE cells recapitulate prostatic histodifferentiation and morphogenesis *in vivo*. H&E staining of wild type UGM+PrE grafts (A) and UGM+Rb-/-PrE grafts (B) that were re-grafted into a male, nude mouse host. Immunohistochemistry revealed (C) AR positive luminal cells and (D) positive staining for the mDLP (E). p63 positive basal cell staining in the UGM+PrE grafts (E) and UGM+Rb-/-PrE grafts (F).

Figure 5. Rb-/-PrE cells exhibit functional p107/p130 and p53/p21 pathways. PrE and Rb-/-PrE cells cultured for 5 days at sub-confluent density (SC), in serum-free media (SF) or at high density (HD) for 5 days were analyzed for levels of (A) p107 protein, (B) p130 protein and (C) an E-cadherin loading control by Western blot. PrE and Rb-/-PrE cells were UV-irradiated, harvested at 48 hours and protein lysates were prepared. Shown are the levels of (D) p53 protein, (E) p21 protein and (F) an actin loading control as measured by Western blot.

Figure 6. Growth kinetics of PrE and Rb-/-PrE cells. PrE and Rb-/-PrE cells were cultured in 5% serum-containing media or charcoal-stripped (DCC) serum growth. Viable cells were counted utilizing trypan blue exclusion at the days indicated.

Figure 7. Cyclin analysis during re-entry into cell cycle. PrE and Rb-/-PrE cells were cultured in the absence of serum for 10 days. Serum-containing medium was added back at time 0 and the cultures were harvested at the indicated times. Protein lysates were prepared and

analyzed for cyclin E1, D1 and PCNA as compared and reported by Western analysis where Actin (1) is the loading control for cyclin E1, D1 and Actin (2) is the loading control for PCNA.

Figure 8. Flow cytometric analysis of log phase and high-density cultures of wild type and Rb-/-PrE cells. Cell cycle analysis of sub-confluent, log phase (A) PrE and (B) Rb-/-PrE cultures under serum- containing growth conditions. High-density culture (15 days) (C) PrE and (D) Rb-/-PrE in serum-containing media. Flow cytometric analysis was analyzed by multicycle software.

Figure 9. SKY analysis of Rb-/-PrE cells. (A) Metaphase analysis of passage 40 Rb-/-PrE cell line by spectral karyotyping. Arrows show 6 copies of chromosome 19 in an otherwise near triploid cell line (arrows). Asterisk shows recurrent translocation between Y and 17 seen in 20% of cells. (B) CGH analysis showing gains of chromosome 19 and loss of chromosome 4 in passage 40 Rb-/-PrE cells. Computed profiles of chromosome 4 and 19 show the degree of loss or gain, respectively, compared to sex- and age-matched +/+ DNA. Mode value is black line, gain and loss of one copy are depicted as fine green and red lines, respectively. Blue line represents the DNA profile of sample. The green line indicates gains and the red line indicates loss, shown next to idiogram.

Figure 1

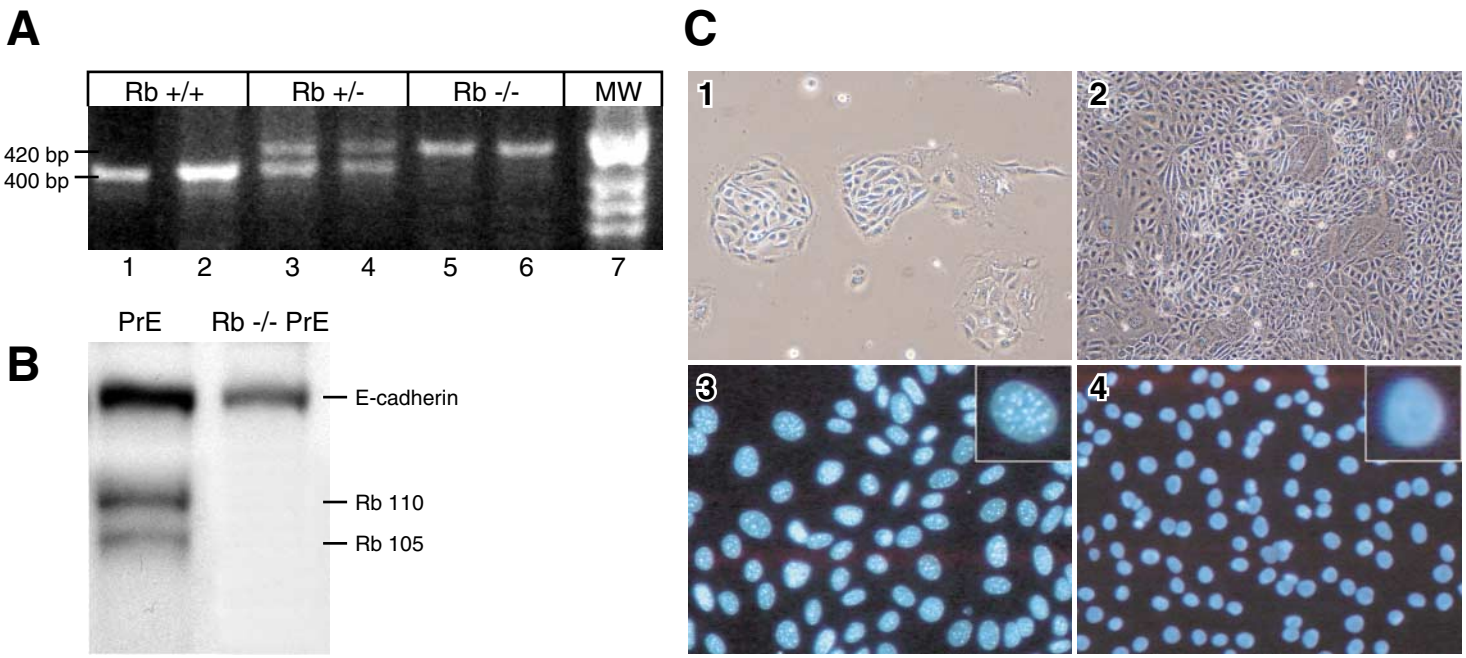
A
Rb +/+
Rb +/-
Rb -/-
MW
420 bp
400 bp
1 2 3 4 5 6 7
B
PrE
Rb -/- PrE
E-cadherin
Rb 110
Rb 105
C
1
2
3
4

Figure 2

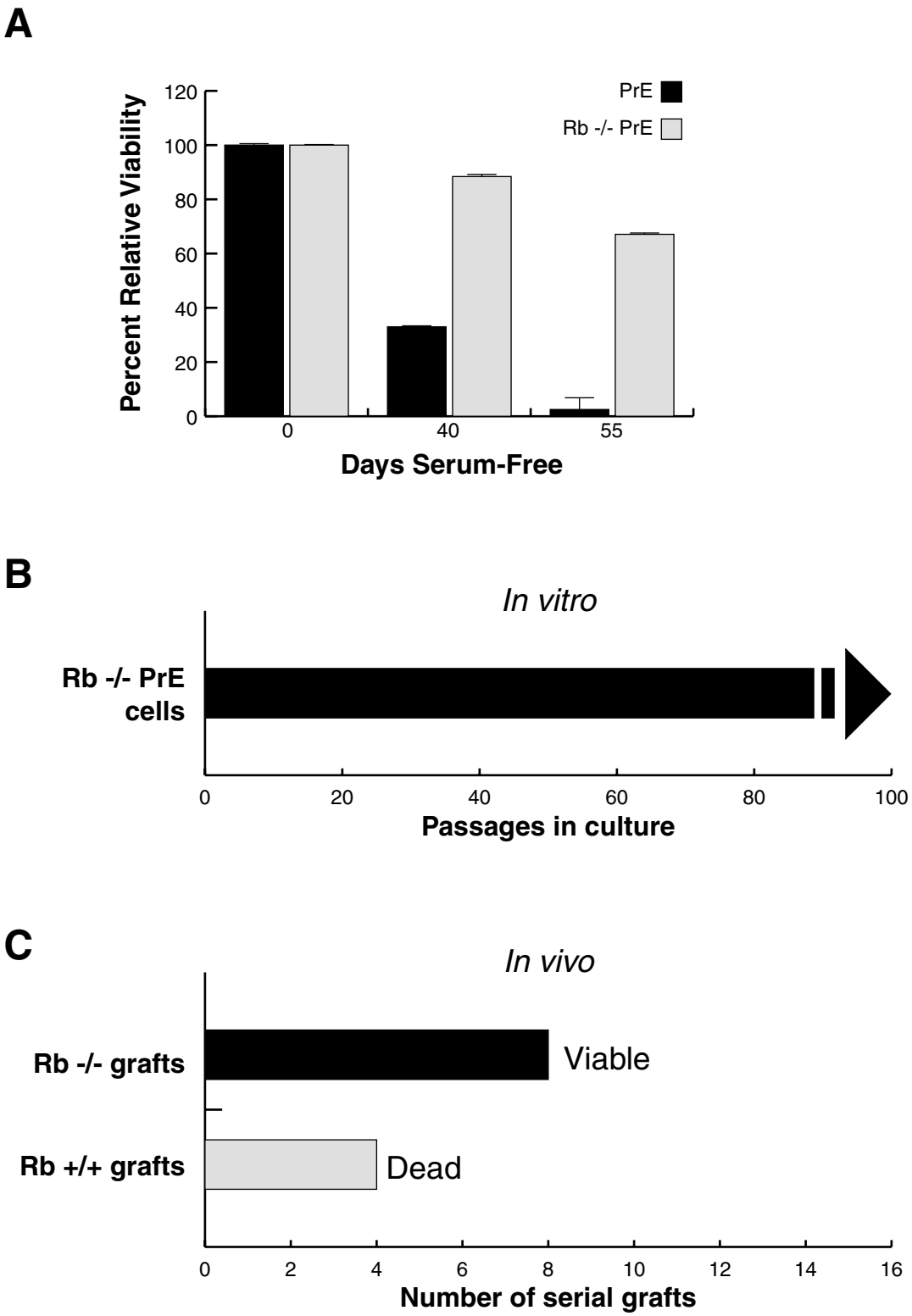
A
Percent Relative Viability
120
100
80
60
40
20
0
PrE
Rb -/- PrE
0
40
55
Days Serum-Free
B
In vitro
Rb -/- PrE cells
0
20
40
60
80
100
Passages in culture
C
In vivo
Rb -/- grafts
Viable
Rb +/+ grafts
Dead
0
2
4
6
8
10
12
14
16
Number of serial grafts

Figure 3

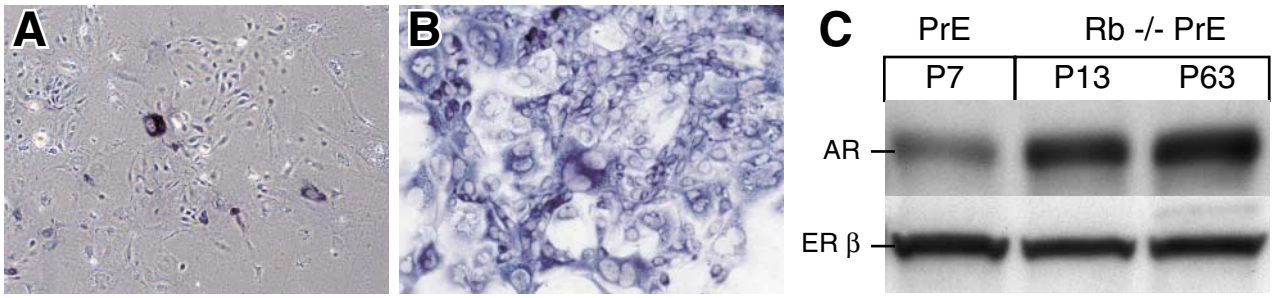

Figure 4

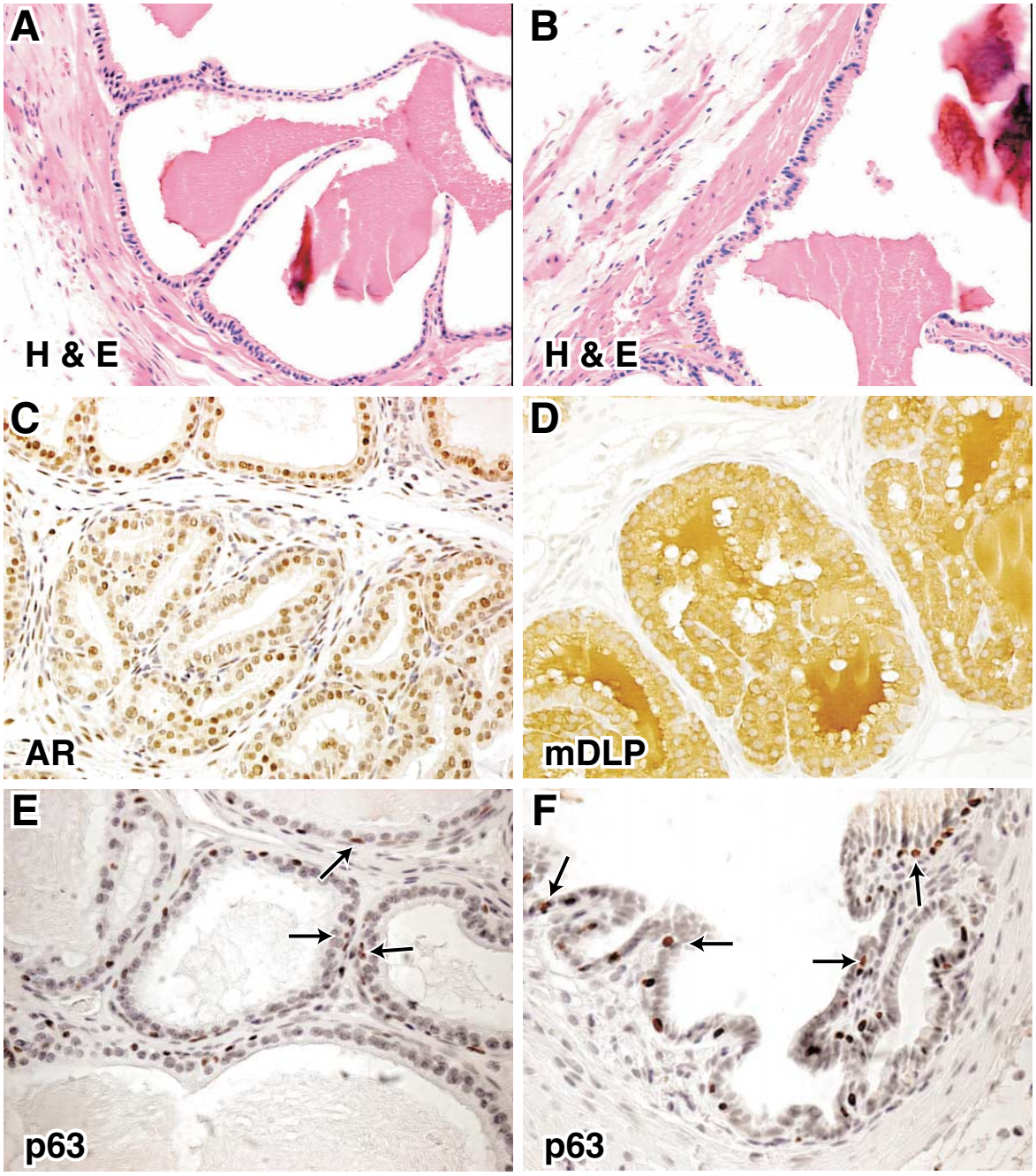

Figure 5

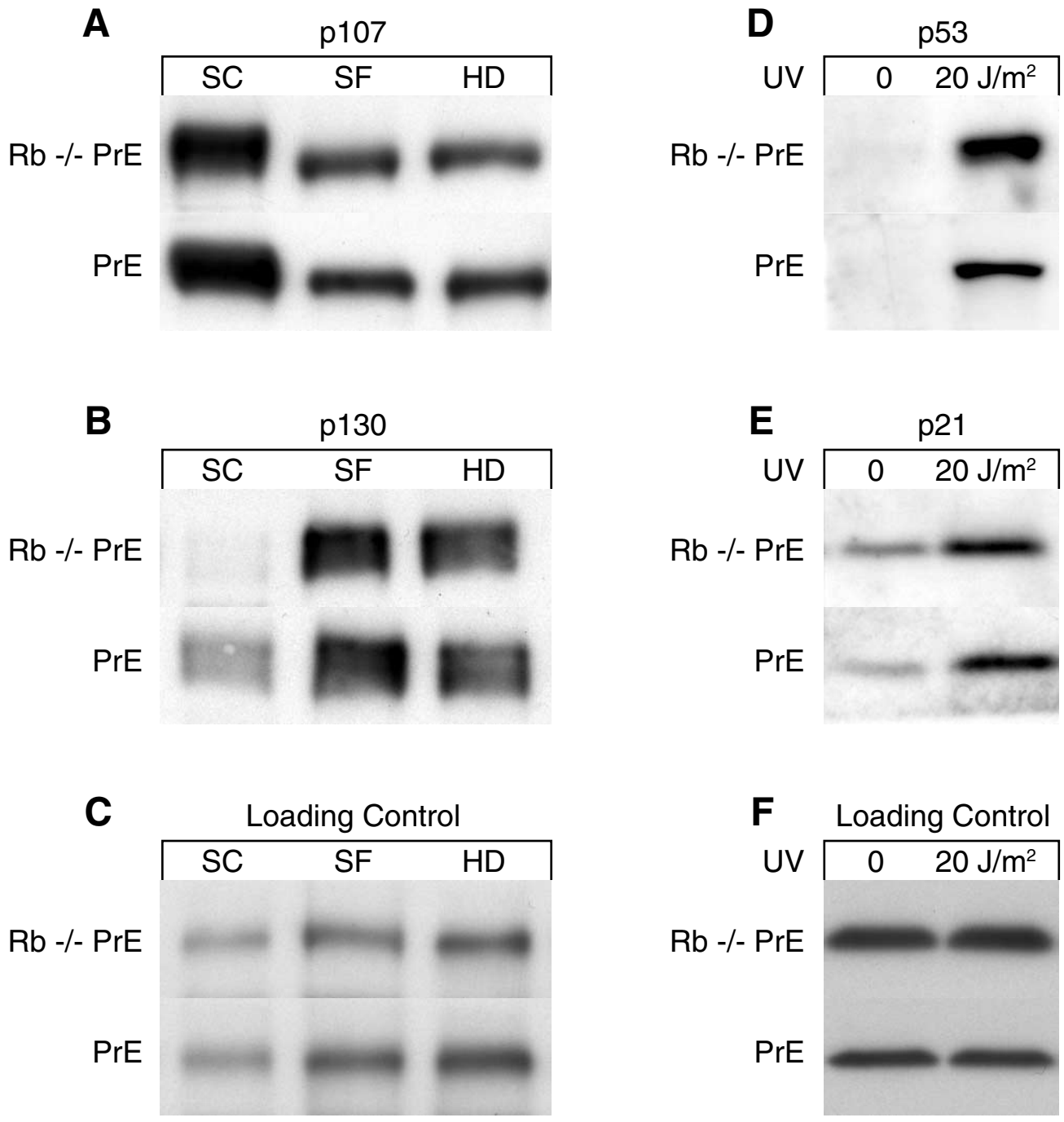
A
p107
SC
SF
HD
Rb -/- PrE
PrE
D
p53
UV
0
20 J/m2
Rb -/- PrE
PrE
B
p130
SC
SF
HD
Rb -/- PrE
PrE
E
p21
UV
0
20 J/m2
Rb -/- PrE
PrE
C
Loading Control
SC
SF
HD
Rb -/- PrE
PrE
F
Loading Control
UV
0
20 J/m2
Rb -/- PrE
PrE

Figure 6

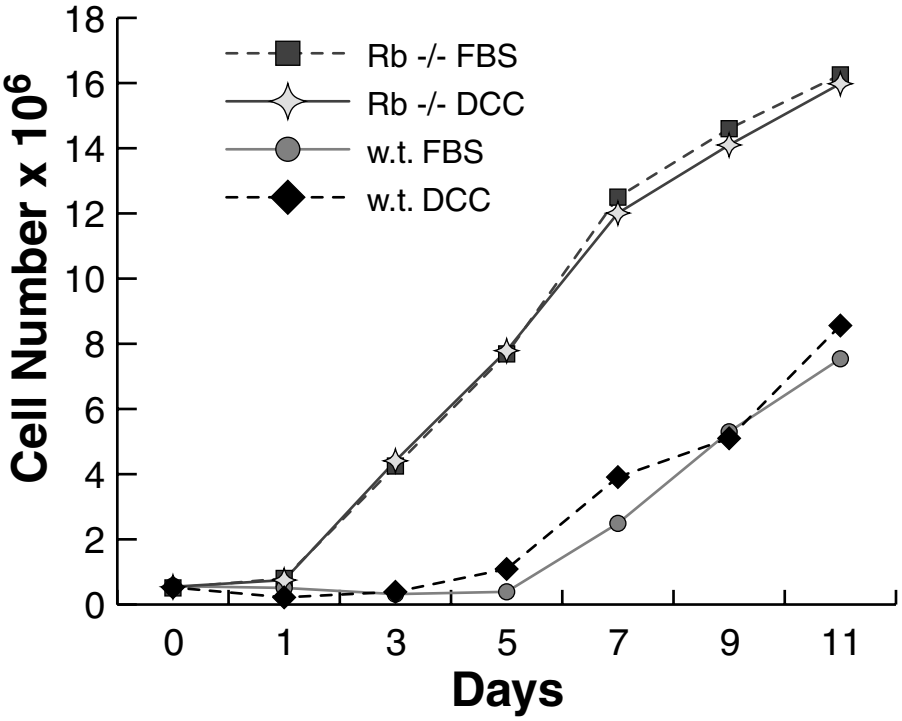
Cell Number x 10^6
18
16
14
12
10
8
6
4
2
0
Rb -/- FBS
Rb -/- DCC
w.t. FBS
w.t. DCC
0
1
3
5
7
9
11
Days

Figure 7

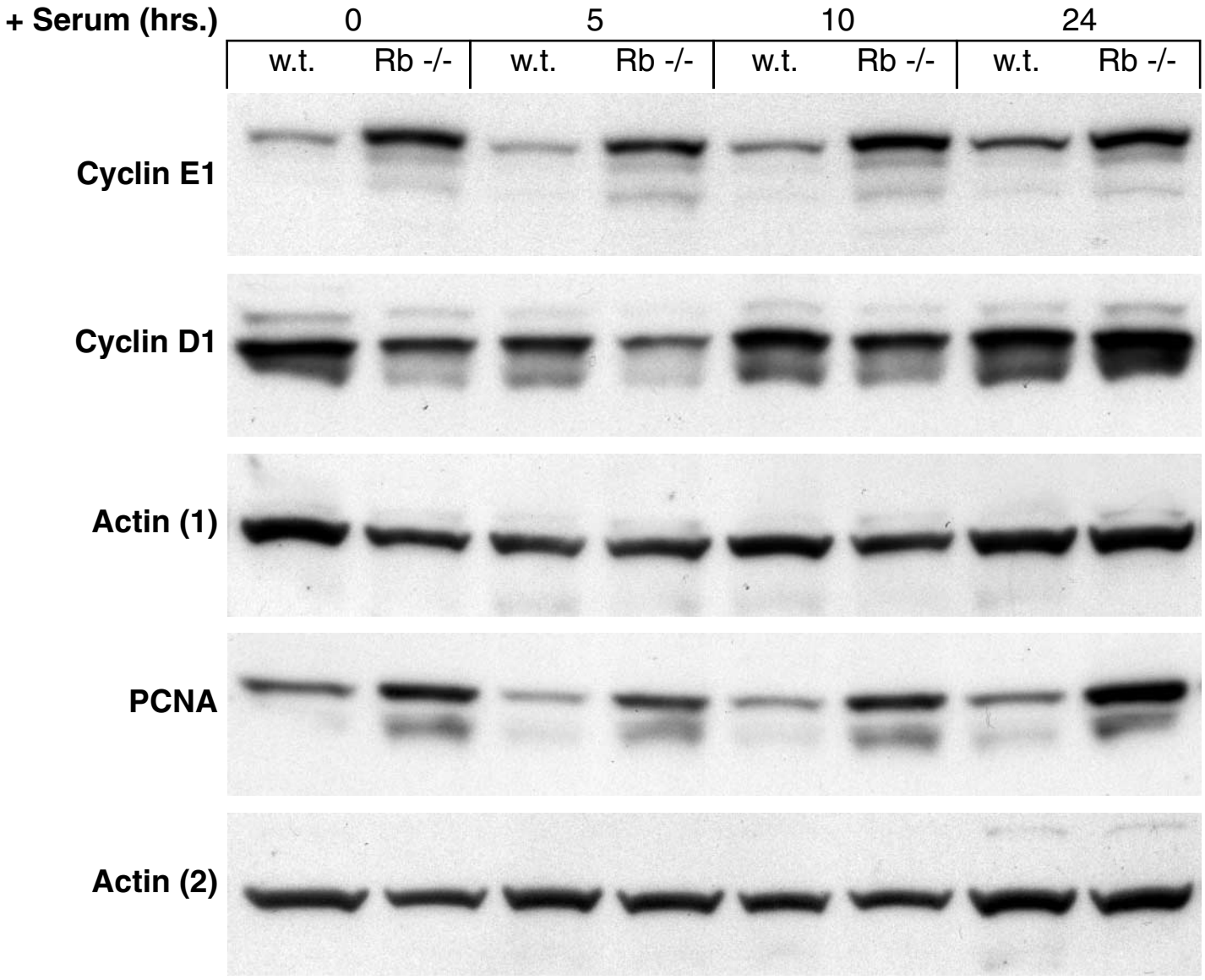
+ Serum (hrs.)
0
5
10
24
w.t.
Rb -/-
w.t.
Rb -/-
w.t.
Rb -/-
w.t.
Rb -/-
Cyclin E1
Cyclin D1
Actin (1)
PCNA
Actin (2)

Figure 8

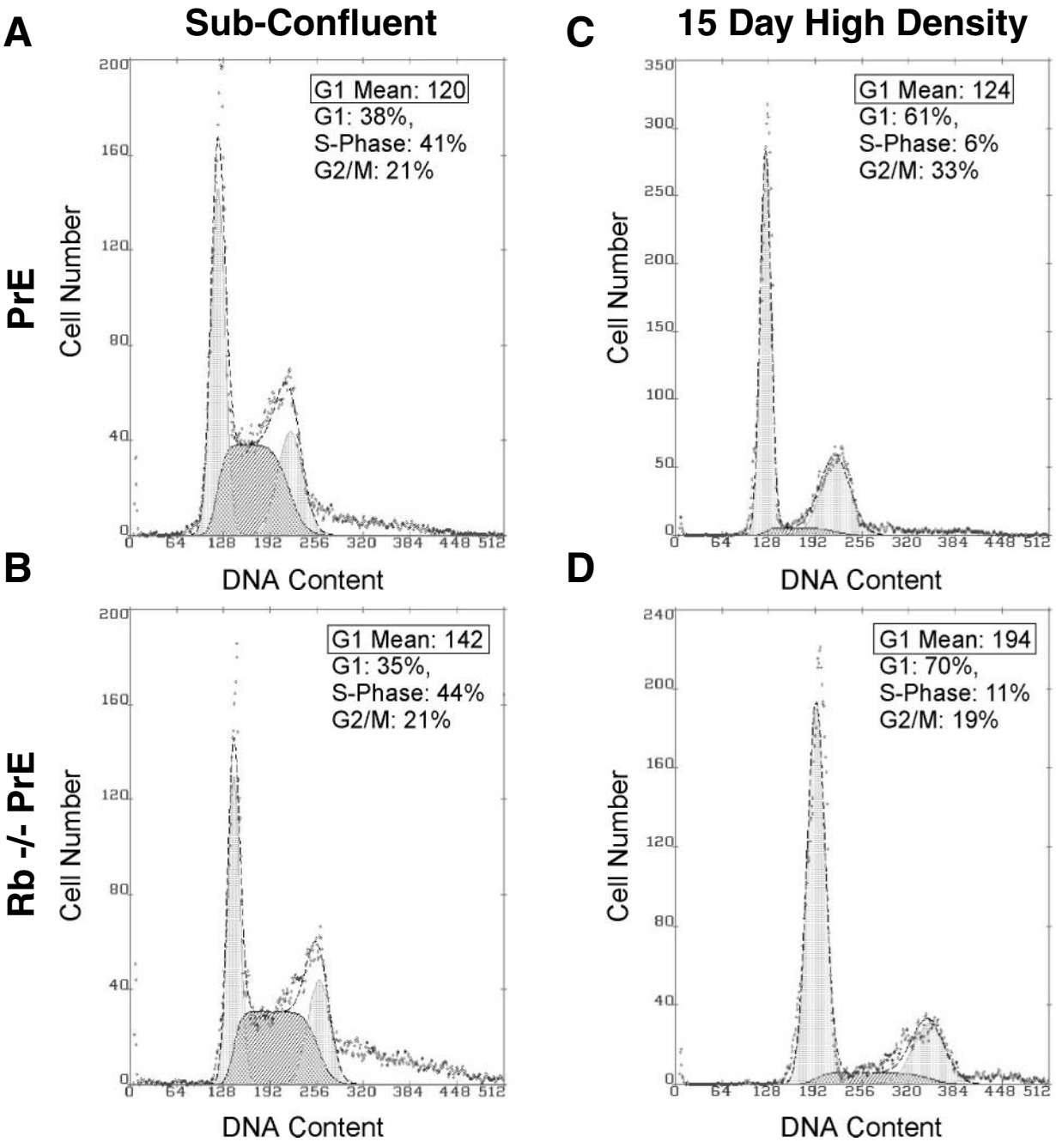
A
Sub-Confluent
C
15 Day High Density
PrE
G1 Mean: 120
G1: 38%,
S-Phase: 41%
G2/M: 21%
G1 Mean: 124
G1: 61%,
S-Phase: 6%
G2/M: 33%
Cell Number
DNA Content
B
D
Rb -/- PrE
G1 Mean: 142
G1: 35%,
S-Phase: 44%
G2/M: 21%
G1 Mean: 194
G1: 70%,
S-Phase: 11%
G2/M: 19%

Figure 9

A

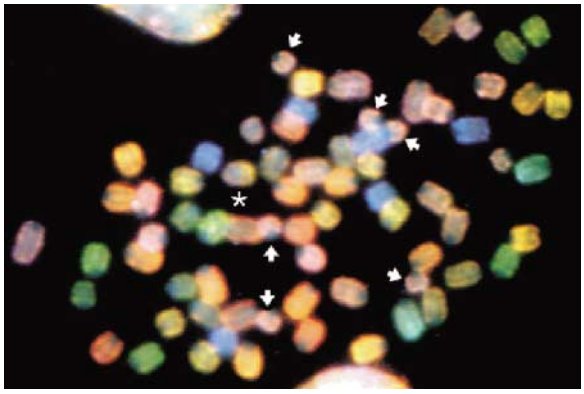

SKY: +19 (x2)

B

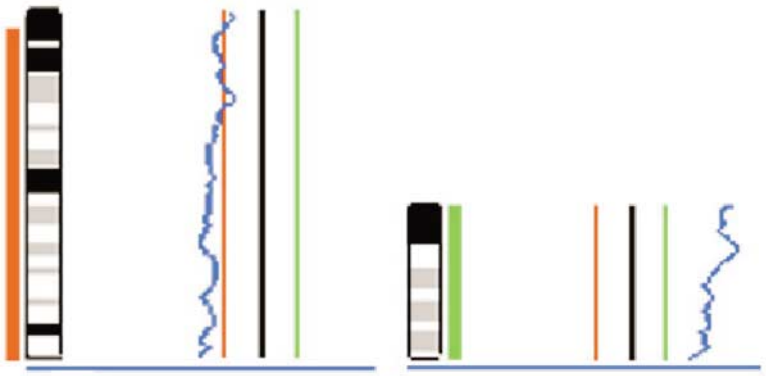

CGH: RB-/- vs RB +/+